National Spherical Torus Experiment Memorandum

Spatial and Photometric Calibration of NSTX line-scan CCD cameras

V. A. Soukhanovskii [1]

Princeton Plasma Physics Laboratory, Princeton, NJ 08543, USA

March 2003

Abstract

Two self-scanning spectrally filtered Dalsa CCD arrays are used on NSTX for midplane and divertor recycling and impurity profile measurments. The CCD arrays have been spatially and photometrically calibrated. Calibration techniques and procedures are summarized and the results of the FY'2002 calibration campaign are presented.

[1] Email address: vlad@pppl.gov

1 Introduction

Two Dalsa CL-C6-2048T cameras have been fielded at NSTX for quantitative measurements of one dimentional (1D) impurity and deuterium brightness profiles. Details of cameras setup and operation can be found in Ref. [1]. This report describes in detail the techniques used for spatial and photometric calibrations of the cameras. The goal is to summarize all relevant information and calibration data so that an independent evaluation of the calibration procedures and results can be performed.

The cameras are operated with several accessories. These are the Kodak wratten neutral density filters, the Barr Associates Inc. interference filters and the Nikon F-mount lenses (see Table 1). Figure 1 shows a photograph of the camera and gives the relevant camera parameters. The camera photometric responsivity curve supplied by Dalsa is presented in Figure 2. The cameras are referred as to the LDIV CCD camera and the MID CCD camera. The former is mounted at Bay E top flange window and views the lower divertor area radially. The latter is mounted in the midplane on Bay I window with a horizontal view across the center stack (Figure 3). The MID CCD operated at Bay B location with the same view prior to the FY'2003 run campaign.

2 Spatial calibration

2.1 General technique description

Both cameras are mounted using rigid G-10 plate structures mechanically referenced to the vacuum vessel port flanges. Some parts of the mounts remain attached to the machine and some parts remain attached to the cameras at all times, so that the camera alignment and spatial calibration relies only on the mechanically referenced surfaces between these parts. The spatial calibration of the cameras usually takes place once per run campaign during a yearly maintanace outage. The calibration requires several hours of manned entry into the NSTX vacuum vessel. After the calibration the cameras are removed from the machine because of the high temperature bake-out conditioning that takes place before plasma operations. The spatial calibration itself involves mounting a number of small lights ("Christmas lights") on the center stack and lower divertor plates and measureing the light positions with a computerized robotic measurment arm. Snapshots of the lights with known positions taken by a camera complete the calibration. A functional dependence between camera pixels and precisely located points on the machine surface viewed by the camera constitutes the calibration. The spatial calibration is performed

without neutral density or interference filters with the lens F-number typically used in experiments. Shown in Figure 4 are the AutoCAD drawings produced by the computerized robotic measurment arm system. Calibration light locations are shown by crosses. Also shown is a photograph of the lower divertor area with the mounted calibration lights.

2.2 Magnification and resolution

Each CCD array has 2048 elements (pixels). The pixel size is 13 μm $\times$500 μm. Camera magnification is defined as a ratio of the image size to the object size. The image size is defined by pixel linear dimentions. From the lens equation we obtain

$$m = \frac{Image}{Object} = \frac{f}{L - f} \tag{1}$$

where f is the lens focal length and L is the distance to object. Using the average typical values of $L_{MID} = 1.40$ m for the MID CCD camera, and $L_{LDIV} = 3.40$ m for the LDIV CCD camera, and $f = 85$ mm we obtain the magnifications as follows: $m_{MID} = 0.064$, and $m_{LDIV} = 0.026$. These values correspond to the radial resolution of the $\rho_{MID} = 0.2$ mm and $\rho_{LDIV} = 0.5$ mm. The resolution of the LDIV camera in the toroidal direction $\vec{\phi}$ is 19 mm. The resolution of the MID CCD camera in the vertical $\vec{z}$ direction is 8 mm.

2.3 LDIV CCD

Shown in Figure 5 is a ray-tracing diagram obtained using the measured LDIV camera and calibration light locations in the lower divertor. Shown in Figure 6 is an LDIV CCD image of the calibration lights. Measured light locations on the CCD array are shown above each peak. The data for the fifteen calibration lights has been fitted with a third degree polynomial as shown in Figure 7. The third degree polynomial was found to approximate the data better than a straight line or a lower/higher degree polynomial. The fitting coefficients are incorporated into an IDL code used for camera data extraction so that the code returns the spatially calibrated data. Note that a major radius coordinate is used to represent the measured divertor profiles. Table 2 summarizes the calibration data. It also contains the Z coordinate which may be needed for precise ray-tracing of divertor brightness profiles modeled by edge transport codes such as UEDGE. The camera "vortex" location is at $R = 1.102$ m and $Z = 1.749$ m. The coordinates used for modeling prior to this calibration were $R = 1.105$ m, $Z = 1.762$ m.

2.4 MID CCD

Shown in Figure 8 is a ray-tracing diagram obtained using the measured MID camera and calibration light locations on the center stack. The Z coordinate is assumed to be zero since the camera and the lights are in the midplane. An impact parameter p was calculated from geometrical considerations for each line of sight connecting the idealized camera point location and each calibration light position. These data are presented in Figure 9 and summarized in Table 3. The best approximation of the correspondence between the calculated impact parameters and peak images on the CCD array was found to be linear. This function is shown in Figure 10. The fitting coefficients are incorporated into an IDL code used for camera data extraction so that the code returns the spatially calibrated data. The brightness profiles as a function of impact parameter are easily inverted using an algebraic inversion algorithm. (To be added at a later time).

3 Photometric calibration

3.1 General technique description

The photometric calibration of the cameras is performed using the LabSphere URS-600 Integrating Sphere Radiance Standard. The source is re-calibrated every year by a LabSphere, Inc. personnel using NIST traceable standards. The present certificate of calibration was issued on the 30th of October 2002. Shown in Figure 11 is the calibration certificate curve as per LabSphere report 37456-1. The calibration was obtained with the luminance value of 43170 foot-lamberts. The measured values are also given in Table 4. The integrating sphere provides a uniform stationary light source. The calibration is performed with an appropriate interference filter, thus the calibration source may be regarded as being monochromatic with the FWHM $\Delta\lambda$ of the filter bandpass $\Delta\lambda = 1.6$ nm. The total flux incident on each CCD pixel of area A (expressed in m^2) is

$$\Phi_p = R_{IS} A_p \Omega \tag{2}$$

where R_{LS} is the LabSphere integrating sphere radiance expressed in Watts/m^2 sr Å, and Ω is the projected solid angle of each pixel's field of view. The latter is determined by the F-number of the lens $F/\# = f/d$, where f is the lens

focal length and d is the lens iris diameter. Therefore

$$\Omega = \frac{\pi d^2}{4f^2(1+m)^2} = \frac{\pi}{(2F(1+m))^2} \tag{3}$$

where m is the camera magnification. The magnification m is usually small and can be neglected. The expression for the irradiance in units of Watt/m^2 becomes

$$E_p = \frac{R_{IS}\pi\epsilon}{(2F(1+m))^2} \tag{4}$$

where ϵ is an optical system efficiency. The latter quantity is assumed to be $\simeq 0.92$, since the Nikon lenses are anti-reflection coated, and 4 % of the incident light is reflected from each surface of the port window. The actual transmission of the port window has not been measured. The monochromatic spectral radiance R_{LS} is determined according to Figure 11 and Table 4. The interpolated value of R_{LS} for $\lambda = 656.1$ nm is 282.932 mW/cm^2/sr/μm.

The photometric calibration of both cameras has been obtained in a laboratory setup for a full field of view. It was not possible to calibrate the cameras *in situ*, mounted on NSTX vacuum vessel. Each camera was setup and aligned with a He-Ne laser as shown in Figure 12. The distance between the camera and the LabSphere integrating sphere opening was established to resemble as close as possible the actual NSTX placement. This distance does not play any role in calibration (since the radiance is inversely proportional to the solid angle), however the actual distance was used to attempt to account for angular attenuation of interference filters. The data was taken at several angular positions of the camera, and was corrected for a geometric cosine factor that follows from the Lambert's law. A good vertical and horizontal alignment was necessary since an "object" image corresponding to each pixel (calculated using the magnifications described above) was not negligible in comparison with the LabSphere integrating sphere opening diameter is 1.5" (3.8 cm).

3.2 LDIV and MID camera calibration results

Shown in Figure 13 and Figure 14 is a summary of calibration data for $\lambda =$ 656.1 nm for LDIV and MID CCD cameras, respectively. The URS 600 spectral irradiance was fairly constant during the calibration. The camera calibration factor is not uniform across the CCD array. This is attributed to the variability in the CCD array response.

An example of the calibration factor calculation is reproduced below. The example refers to one of the LDIV CCD central data points (calibration shot 3200069) in Figure 13. The camera measures $I_p \simeq 1200$ counts (background subtracted) at a rate of 4800 frames/s (lines/s). The LabSphere luminance at the time of measurements was 7590 ft lamberts (background subtracted). This corresponds to the radiance of $R \simeq 4.976 \times 10^{-6}$ W/cm^2/sr which follows from Figure 11:

$$R = \frac{7590 ft\ lamberts \ \times \ 282.93\ mW/cm^2/sr/\mu m}{43170 ft\ lamberts} = \tag{5}$$
$$= \frac{7590 ft\ lamberts \ \times \ 2.83 \times 10^{-5}\ W/cm^2/sr/\mathring{A}}{43170 ft\ lamberts} =$$
$$= 4.976 \times 10^{-6}\ W/cm^2/sr/\mathring{A}$$

The CCD array irradiance E_p is calculated according to Equation 4. The F-number is 1.8, and the filter FWHM $\delta\lambda = 16$ Å.

$$\eta = \frac{E_p(LS)}{I_p(counts)} = \frac{R\,\pi\,\epsilon}{(2F(1+m))^2\ I_p} = \tag{6}$$
$$= \frac{4.976 \times 10^{-6}\ W/cm^2/sr/\mathring{A}\ \ \pi\ \ 0.68\ \ 16.0\mathring{A}}{(2 \cdot\ 1.8\ \cdot 1.026)^2\ \ 1200.} =$$
$$= 1.53 \times 10^{-8}\ \frac{W}{cm^2\ count}$$

Each watt of irradiance at $\lambda = 656.1$ nm corresponds to 3.30535×10^{18} photons/s. We obtain

$$\eta = 1.53 \times 10^{-8}\ \frac{W}{cm^2\ count}\ \times 3.31 \times 10^{18} = 5 \times 10^{10} \frac{photons}{s\ cm^2\ count} \tag{7}$$

In order to obtain plasma D_α brightness into 4 π the solid angle of the actual F-number lens must be used again. The plasma irradiance into 4 π for $F = 1.8$ then is

$$\eta = 5 \times 10^{10} \frac{photons}{s\ cm^2\ count} \times \frac{4\ \pi}{\Omega_F} = 5 \times 10^{10} \times \frac{4\ \pi}{0.242} = \tag{8}$$
$$= 5 \times 10^{10} \times 51.84 = 2.6 \times 10^{12} \frac{photons}{s\ cm^2\ count}$$

For a typical divertor D_α brightness of 1000 - 4000 counts and the neutral density filter attenuation of 10^3 we obtain $B_{D_\alpha} \leq (0.2-1) \times 10^{23}$ photons/s/m^2.

It is possible to cross-check the laboratory photometric calibration of the cameras using the estimates derived from the camera responsivity curve shown in

Figure 2. The curve yields the pixel responsivity in units of counts/(nJ/cm^2, from which the pixel irradiance E_p (in units of Watt/m^2) and the object spectral radiance R_{LS} can be estimated according to Equation 4. At $\lambda = 656.1$ nm the camera responsivity is ~ 610 counts/(nJ/cm^2). Suppose the camera is operated at a scan rate 4.8 kHz, which corresponds to an integration time of 0.208 ms. Therefore, the CCD array irradiance is

$$E_p = \frac{1}{610\ counts/(nJ/cm^2)} \times \frac{1}{0.208\ ms} = 7.88 \times 10^{-9}\ \frac{W/cm^2}{count} \qquad (9)$$

During the calibration we recorded $I \simeq 1200$ counts, or $E_p = 9.46 \times 10^{-6}$ W/cm^2. The object radiance is

$$R_{LS} = \frac{E_p\ (2F(1+m))^2}{\pi\ \epsilon} = \qquad (10)$$
$$= \frac{9.46 \times 10^{-6}\ \ (2 \cdot\ 1.8\ \cdot 1.026)^2}{\pi\ \ 16.0} = 2.6 \times 10^{-6}\ \ W/cm^2/sr/\mathring{A}$$

The derived radiance is a factor of 2 smaller than the radiance actually used in the calibration, as measured by the LabSphere calibrated silicon diode. It has not been possible to resolve this discrepancy at this time. The camera calibration with the URS 600 source has been performed several times over a period of over one year, before and after the URS 600 source was re-calibrated at LabSphere, Inc. These calibrations have produced consistent results. Therefore, it has been concluded that the camera responsivity provided by Dalsa gives only a nominal responsivity value.

3.3 Relative responsivity calibration

Shown in Figure 15 is an in-vessel view of the MID CCD camera mounted at Bay I. The 6" diameter window provides a clear view of the center stack. The in-vessel photograph of the LDIV CCD camera is shown in Figure 16. An attempt was made to assess the extent of possible vignetting of the port and passive plates on the LDIV camera field of view. Several images of an H_α lamp were taken by LDIV CCD camera mounted on the port and operated in conditions resembling the experimental ones. The test revealed that LDIV camera responsivity is variable across the field of view, being the most sensitive in the center of the array and falling off toward the edges, similar to the results from the photometric calibration. The quantitative assessment of the *in situ* responsivity measurement was hampered by the non-stationary behavior of the H_α lamp light. A white plate or a LabSphere *in situ* responsivity calibration should be considered in the future.

3.4 Effects of focusing

Measurements were conducted to assess the effects of camera focusing on the irradiance (brightness) measurements. Shown in Figure 17 are the LabSphere 1.5" opening irradiance profiles measured by the LDIV camera located at a distance of 3.30 m (the nominal distance between the camera and the NSTX divertor plates). As can be seen, a well focussed camera produces a profile of about 75 pixels wide, which corresponds to 38 mm object size using the magnification of 0.026. The LabSphere opening diameter is 38.1 mm. It is evident that the camera has an adequate depth of field. Shown in Figure 18 are the LabSphere 1.5" opening irradiance profiles measured by he LDIV camera focussed at 11 ft and located at various distances from the LabSphere source. Contributions from the objects which are out of focus and located close to the camera are comparable to those from the objects which are in focus.

Acknowledgments

A. L. Roquemore and R. Feder are gratefully acknowledged for the operational and engineering support of the described calibration activities. G. Zimmer is acknowledged for the software development. R. Maingi (ORNL) and C. H. Skinner (PPPL) are acknowledged for the comments and critical examination of the calculations in this memorandum. The cameras are property of Oak Ridge National Laboratory, Oak Ridge, Tennessee.
This research was supported by the U.S. Department of Energy under contracts No. DE-AC02-76CH03073, DE-AC05-00OR22725.

References

[1] V. A. Soukhanovskii, A. L. Roquemore, C. H. Skinner, J. Menard, H. W. Kugel, D. Johnson, R. Maingi, S. Sabbagh and F. Paoletti, Review of Sci. Instrum. 74 (3) 2094 (2003).

Tables

Lens	
Diameter	75 mm (3 in)
Focal length f	85 mm
Range of F-numbers	1.2 ...16

Interference filter	
Diameter	75 mm (3 in)
Spectral bandpass $\Delta\lambda$	1.0 - 1.5 nm
Transmission at λ_{cwl}	0.5 -0.65

Table 1
Parameters of the camera lens and interference filter

Major radius R (m)	Vertical coordinate Z (m)	Pixel on CCD array
1.1179	-1.587	78
1.082	-1.590	153
1.033	-1.593	254
0.948	-1.593	425
0.907	-1.593	507
0.850	-1.603	618
0.793	-1.583	728
0.736	-1.564	837
0.684	-1.541	932
0.634	-1.519	1024
0.569	-1.496	1154
0.508	-1.479	1269
0.435	-1.447	1407
0.364	-1.424	1545
0.299	-1.321	1666

Table 2
Measured calibration light coordinates used in LDIV CCD camera spatial calibration. The camera "vortex" location is at $R = 1.102$ m and $Z = 1.749$ m.

Horizontal coordinate X (m)	Horizontal coordinate Y (m)	Calculated impact parameter p (m)	Pixel on CCD array
1.781	0.157	0.190	1008
1.764	0.178	0.1720	1065
1.753	0.200	0.1437	1160
1.742	0.228	0.1253	1220
1.738	0.248	0.1018	1300
1.735	0.272	0.0788	1374
1.736	0.297	0.0454	1472
1.740	0.326	0.020	1564
1.747	0.348	-0.006	1655
1.758	0.373	-0.029	1728
1.770	0.393	-0.061	1839
1.804	0.429	-0.086	1923
1.847	0.456	-0.110	2003

Table 3
Measured calibration light coordinates and calculated impact parameters for the corresponding lines of sight used in MID CCD camera spatial calibration.

Wavelength (μm)	Spectral Radiance (mW/cm^2-sr-μm)
0.30	2.11e+0
0.31	3.19e+0
0.32	4.71e+0
0.33	6.71e+0
0.34	9.49e+0
0.35	1.26e+1
0.40	3.96e+1
0.45	8.23e+1
0.50	1.33e+2
0.55	1.92e+2
0.60	2.35e+2
0.655	2.82e+2
0.70	3.17e+2
0.80	3.58e+2
0.90	3.51e+2
1.05	3.19e+2
1.15	2.84e+2
1.20	2.68e+2
1.30	2.35e+2
1.54	1.53e+2
1.60	1.42e+2
1.70	1.12e+2
2.00	4.48e+1
2.10	2.34e+1
2.30	1.72e+1
2.40	1.23e+1

Table 4
Spectral radiance calibration of the LabSphere URS-600 Radiance Standard

Figures

Specifications

Resolution	2048
Pixel Size	13 µm x 500 µm
Aperture	26.7 x 0.5 mm
Lens Mount	F-mount
Max Frame Rate	4.8kHz
Data rate	10 MHz
Data Format	12-bit RS422
Responsivity	618 DN/(nJ/cm^2)
Dynamic Range	1420:1

Fig. 1. Dalsa CL-C6 camera photograph and operating parameters

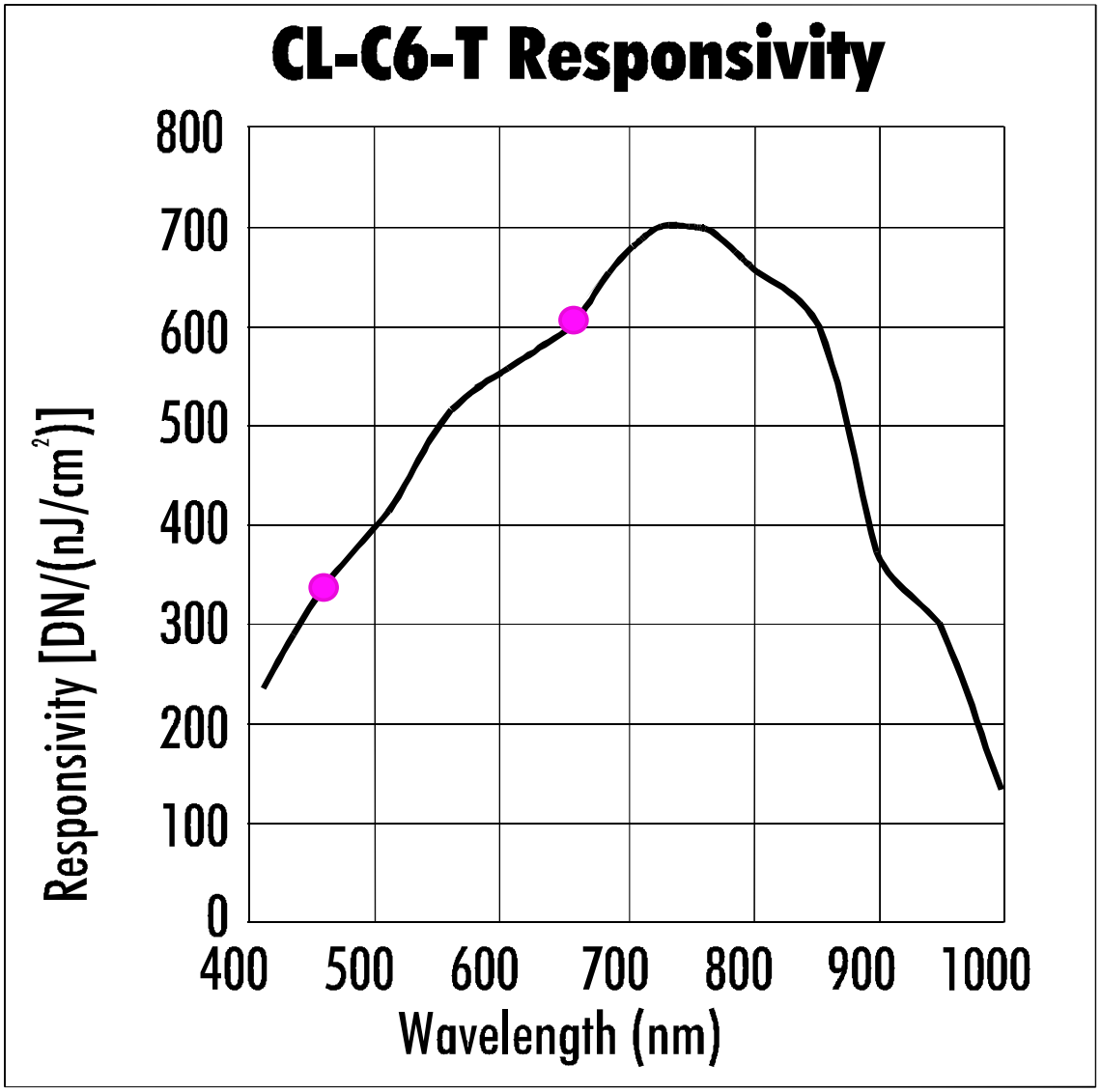

Fig. 2. Dalsa CL-C6 camera responsivity. Shown by filled circles are the locations of $\lambda = 656.1$ nm (D_α and $\lambda = 465.0$ nm (C III).

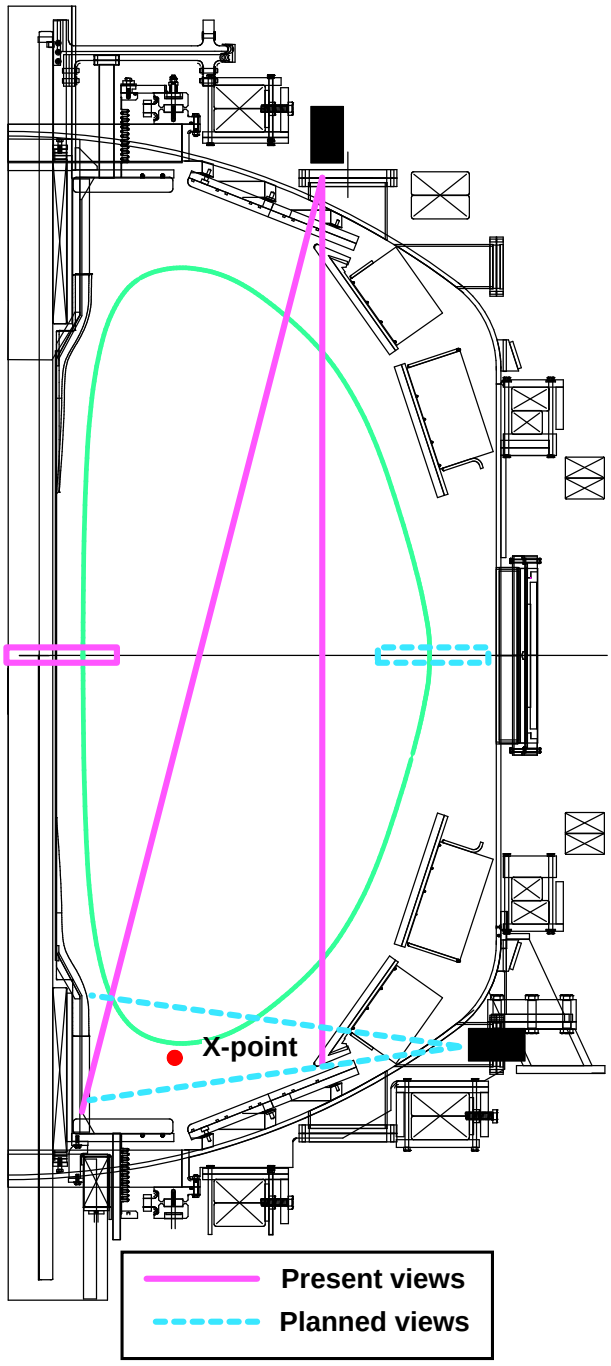

Fig. 3. Dalsa cameras placement on NSTX

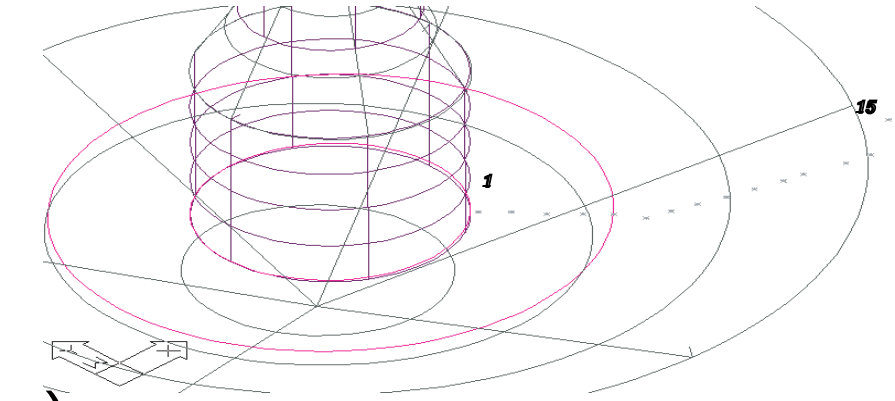

a)

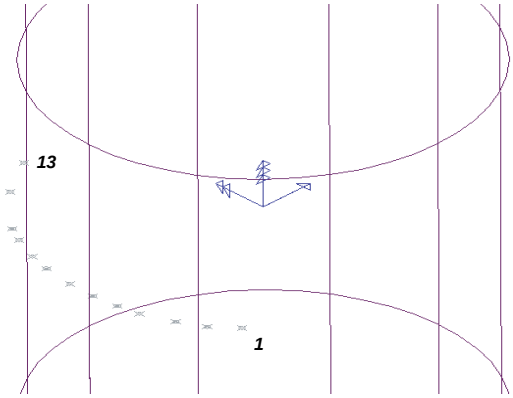

b)

Fig. 4. AutoCAD drawings of calibration ("Christmas") lights positions measured with a robotic measuring arm system for the LDIV camera viewing lower divertor (a) and MID camera viewing the center stack (b).

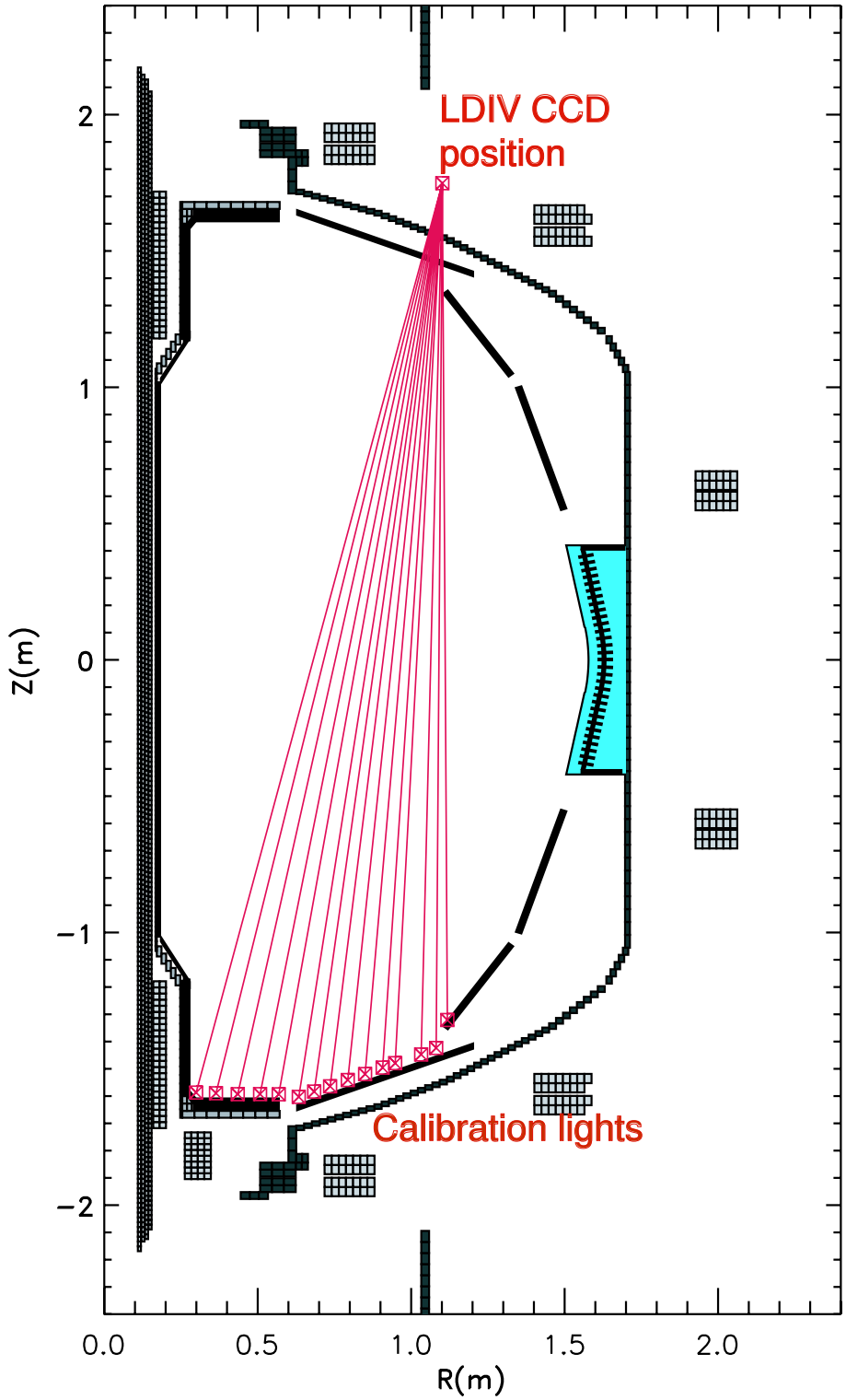

Fig. 5. Bay E top LDIV CCD camera spatial calibration ray-tracing diagram.

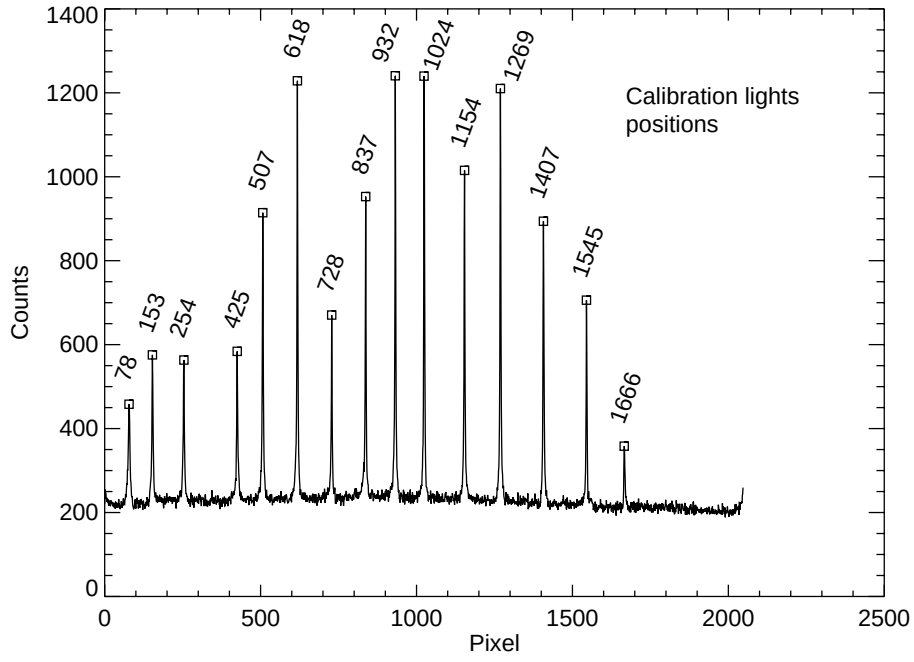

Fig. 6. LDIV CCD image of calibration lights in the lower divertor and individual light image locations on the CCD array.

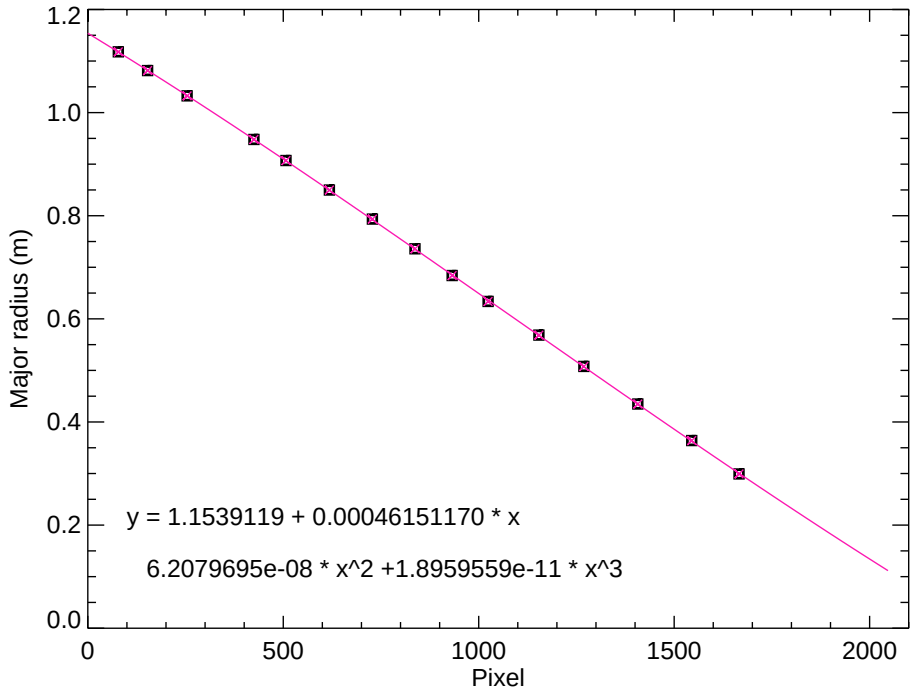

Fig. 7. Spatial calibration of LDIV CCD camera. Each pixel corresponds to a major radius R measured with a computerized robotic arm system.

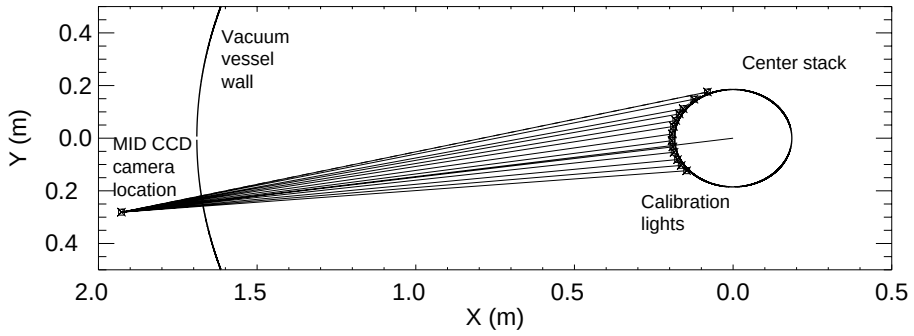

Fig. 8. Bay I MID CCD camera spatial calibration ray-tracing diagram.

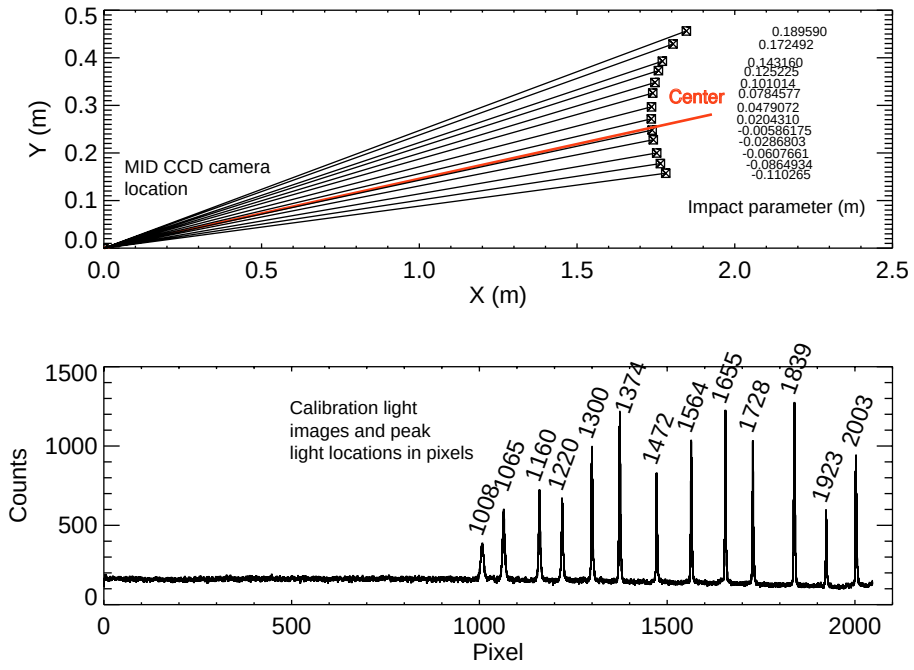

Fig. 9. Spatial calibration of MID CCD camera. (a) - Calculated impact parameters are found from the ray-tracing diagram for each calibration light. (b) MID CCD image of calibration lights and image locations on the CCD array.

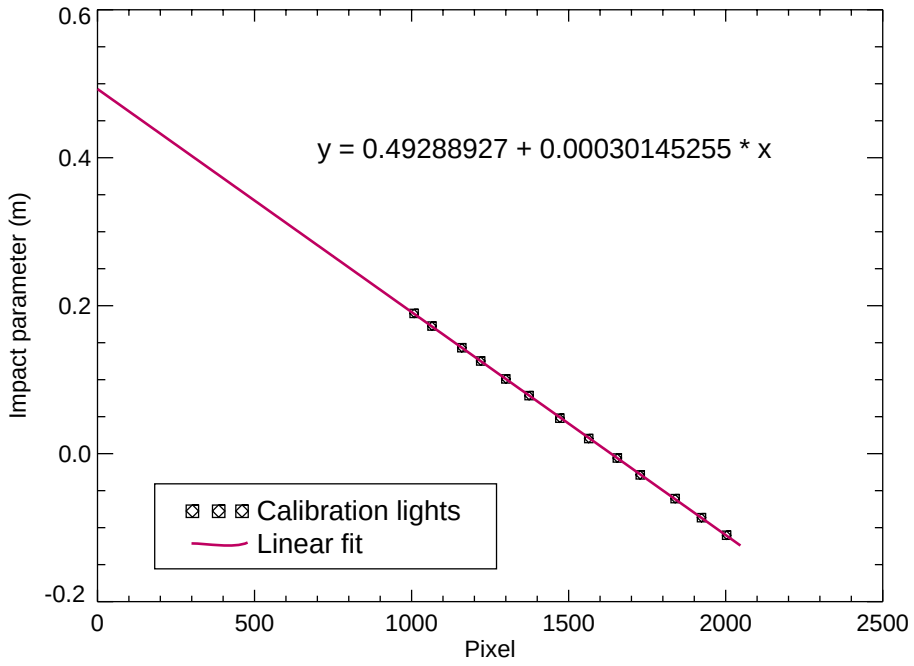

Fig. 10. Spatial calibration of MID CCD camera. Each pixel corresponds to an impact parameter p in respect to the center line connecting the camera location and the geometric center of the vacuum vessel.

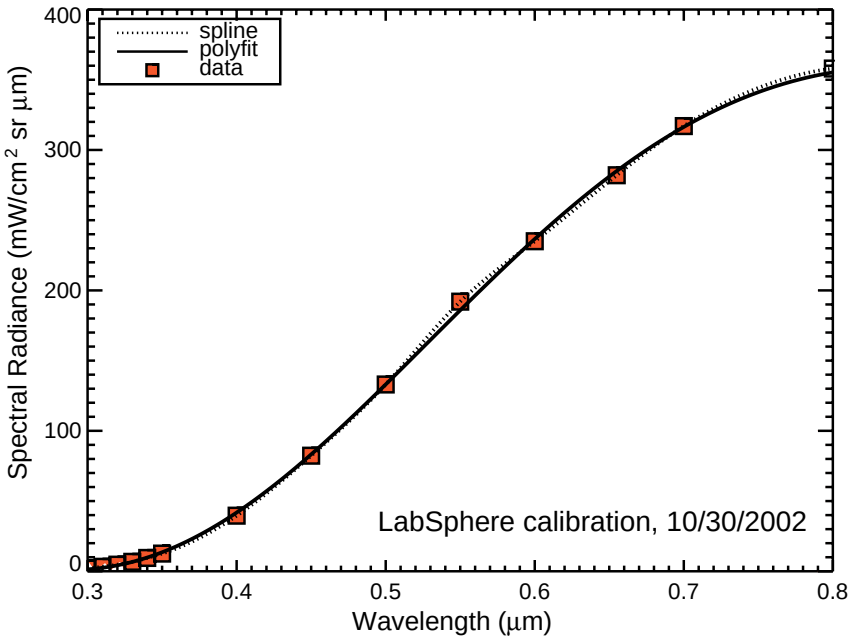

Fig. 11. LabSphere URS-600 Integrating Sphere Radiance Standard spectral radiance curve for 43170 ft-lamberts luminance.

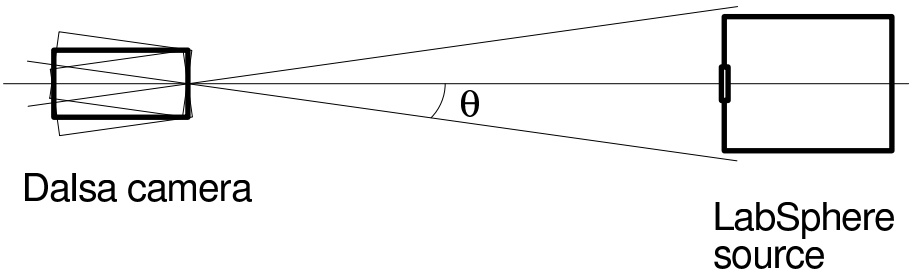

Fig. 12. Calibration setup

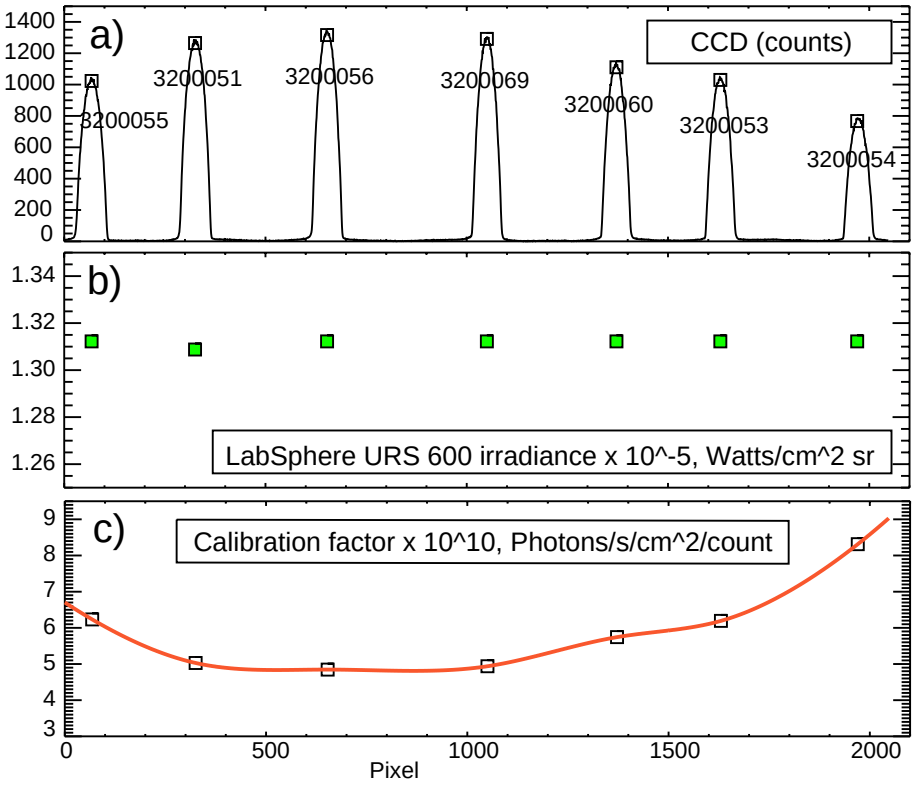

Fig. 13. LDIV CCD camera photometric calibration data. (a) - Images of the LabSphere URS 600 source 1.5" diameter opening. The square symbols indicate average counts for each angular position (image). The numbers indicate calibration shot numbers stored in the MDS Plus system. (b) - LabSphere ERS 600 irradiance for each angular position. (c) - LDIV CCD camera photometric calibration curve for $\lambda = 6561$ Å (D_α).

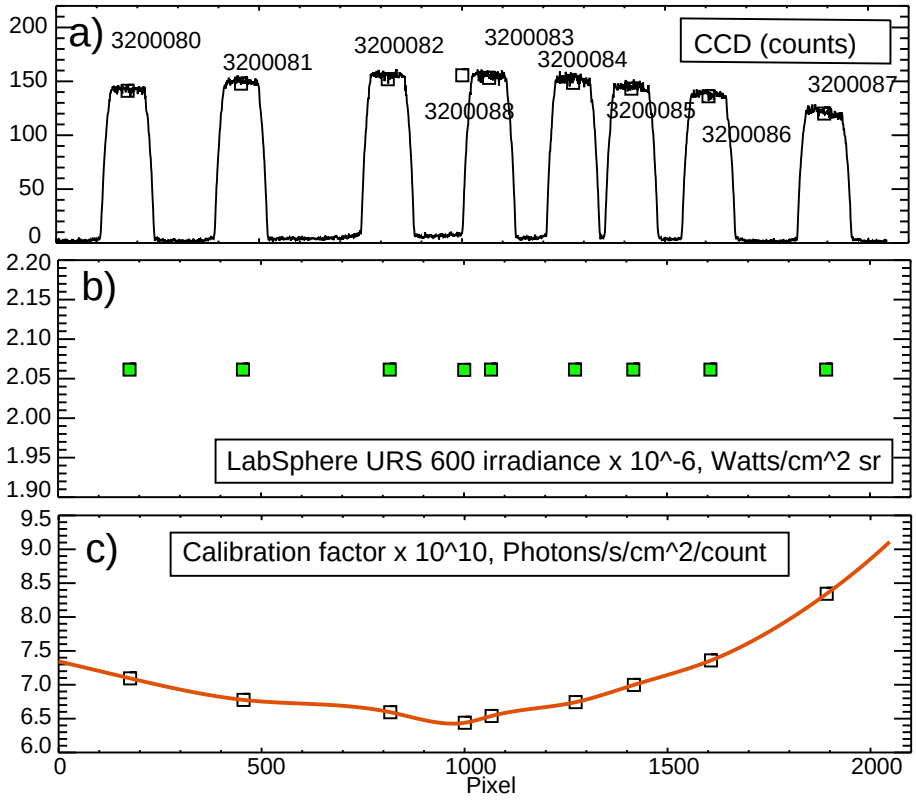

Fig. 14. MID CCD camera photometric calibration data. (a) - Images of the LabSphere URS 600 source 1.5" diameter opening. The square symbols indicate average counts for each angular position (image). The numbers indicate calibration shot numbers stored in the MDS Plus system. (b) - LabSphere URS 600 irradiance for each angular position. (c) - MID CCD camera photometric calibration curve for $\lambda = 6561$ Å (D_α).

Fig. 15. In-vessel view of the MID CCD camera mounted at Bay I port 6" window. Neutral beam armor is on the left.

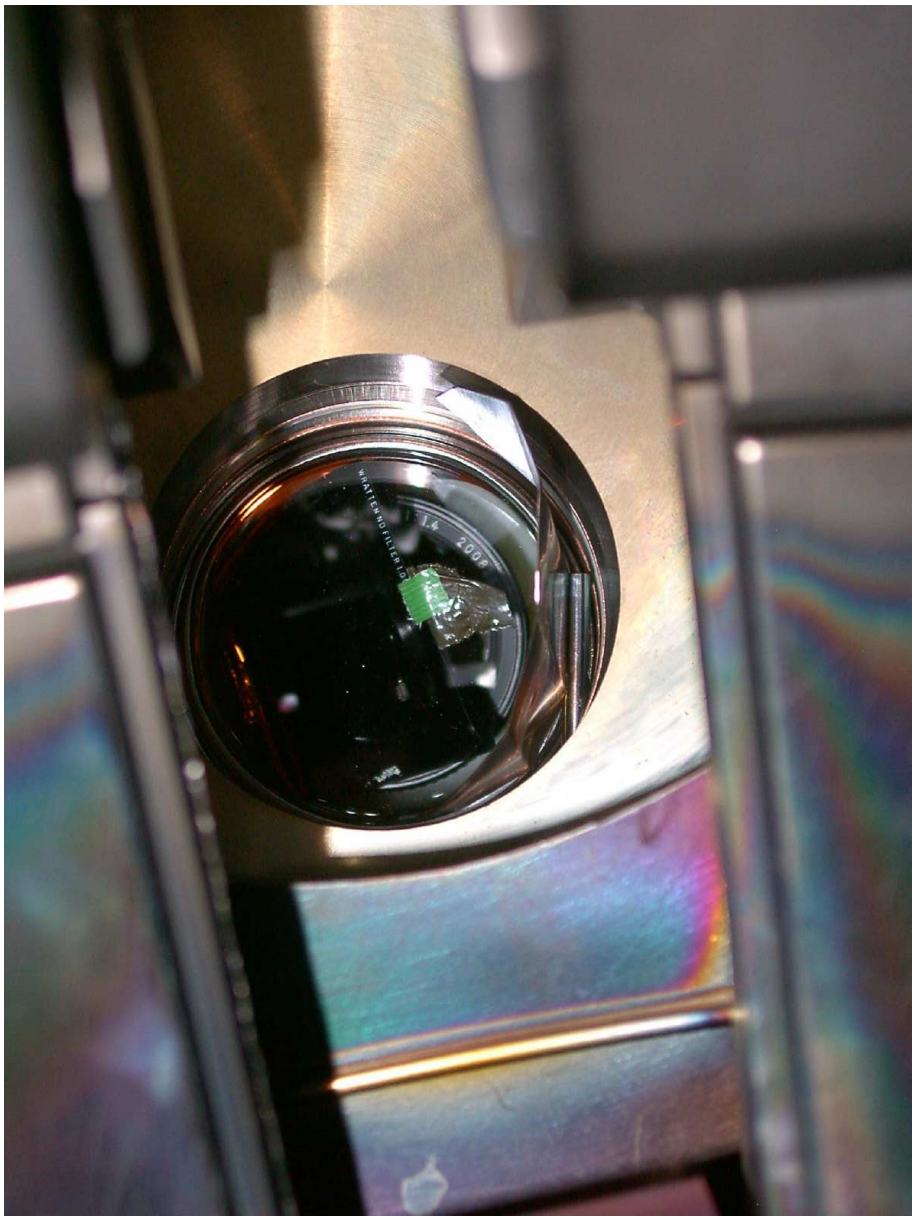

Fig. 16. In-vessel view of the LDIV camera mounted at Bay E top port 4" window. The port is recessed behind the vacuum vessel wall and the stabilizing plates seen on the front.

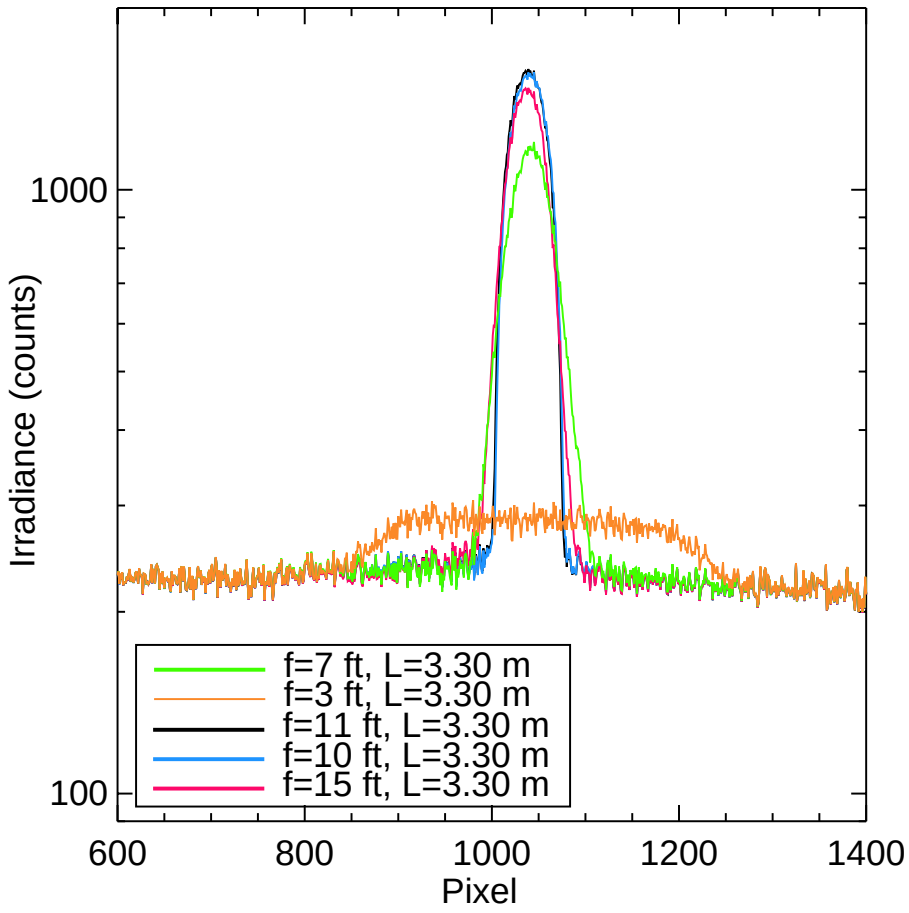

Fig. 17. Irradiance profiles of the LabSphere opening located at $L \simeq 11$ ft $\simeq 3.30$ m from the LDIV camera focussed at different distances

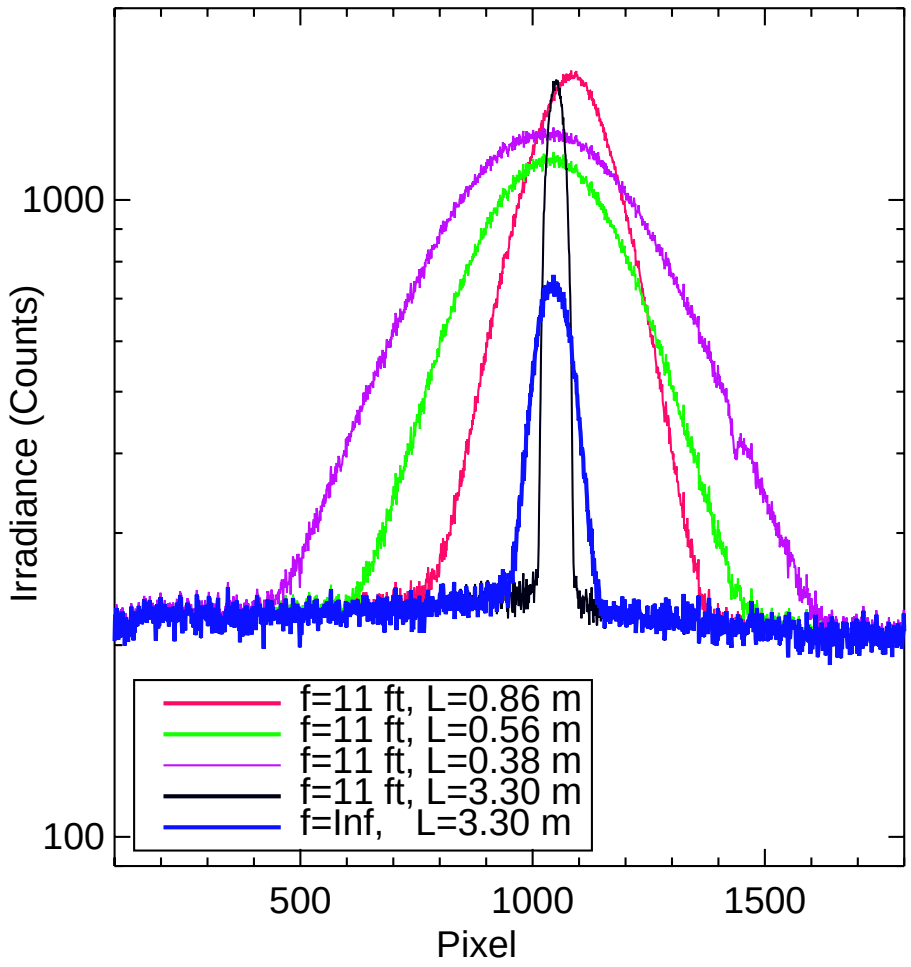

Fig. 18. Irradiance profiles of the LabSphere opening located at different distances from the LDIV camera focussed at 11 ft or infinity